Biochemical and Biophysical Research Communications 391 (2010) 431–436

Contents lists available at ScienceDirect

Biochemical and Biophysical Research Communications

journal homepage: www.elsevier.com/locate/ybbrc

Structural basis for the substrate specificity of PepA from *Streptococcus pneumoniae*, a dodecameric tetrahedral protease

Doyoun Kim [a], Boi Hoa San [a,b], Sang Hyun Moh [a,b], Hyejin Park [a], Dong Young Kim [a], Sangho Lee [c,*], Kyeong Kyu Kim [a,b,*]

[a] Department of Molecular and Cell Biology, Samsung Biomedical Research Institute, Sungkyunkwan University School of Medicine, Suwon 440-746, South Korea
[b] Sungkyunkwan Advanced Institute of Nanotechnology, Sungkyunkwan University, Suwon 440-746, South Korea
[c] Department of Biological Science, Sungkyunkwan University, Suwon 440-746, South Korea

ARTICLE INFO

Article history:
Received 3 November 2009
Available online 13 November 2009

Keywords:
Glutamyl aminopeptidase
PepA
Tetrahedral aminopeptidase
Substrate specificity
M42 family protease
Streptococcus pneumoniae

ABSTRACT

Regulated cytosolic proteolysis is one of the key cellular processes ensuring proper functioning of a cell. M42 family proteases show a broad spectrum of substrate specificities, but the structural basis for such diversity of the substrate specificities is lagging behind biochemical data. Here we report the crystal structure of PepA from *Streptococcus pneumoniae*, a glutamyl aminopeptidase belonging to M42 family (SpPepA). We found that Arg-257 in the substrate binding pocket is strategically positioned so that Arg-257 can make electrostatic interactions with the acidic residue of a substrate at its N-terminus. Structural comparison of the substrate binding pocket of the M42 family proteases, along with the structure-based multiple sequence alignment, argues that the appropriate electrostatic interactions contribute to the selective substrate specificity of SpPepA.

Introduction

Cytosolic proteolysis is critical in regulating cell proliferation, protein maturation, and metabolism [1,2]. Such cytosolic proteolysis is carried out by self-compartmentalized proteases in order to prevent the degradation of unwanted substrates [3]. The cytosolic proteolytic systems can be classified into two pathways: energy-dependent and independent pathways. The energy-dependent proteolysis is employed to degrade proteins that are not needed any more or misfolded [4,5]. In prokaryotes, these substrates are first recognized by unfoldases such as ClpA and ClpX and delivered to the associated protease complexes like ClpP, which then release short oligopeptides [5]. Final processing of the resulting oligopeptides is performed by the energy-independent pathway, liberating free amino acids. One of such proteases involved in the energy-independent pathway is a hexameric protease complex from *Thermoplasma acidophilum*, named as the tricorn protease (TRI) [6]. TRI digests oligopeptides generated by the energy-dependent proteases to di- or tri-peptides. TRI interacts with its interacting factors, such as F1, F2, and F3, yielding free amino acids [7].

Recently, a novel energy-independent protease complex from the archaeon *Haloarcula marismortui*, HmTET, has been identified [8]. It is called tetrahedral (TET) protease due to its oligomeric architecture. TET protease is self-compartmentalized to restrict the entry of substrates by length of oligopeptides [8]. The crystal structures of TET protease from *Pyrococcus horikoshii* revealed the tetrahedral architecture comprises of 12 subunits and that all the active sites are located in the central cavity [9,10]. The TET proteases have been shown to cleave short peptides in a metal-dependent manner. Biochemical and structural studies of three TET proteases, PhTET1, PhTET2, and PhTET3, from *P. horikoshii* shed light on functionally diverse bacterial proteolytic pathway. Although they share a similar fold, their functions are distinct due to their different substrate specificities [11–13]. TET proteases belong to the M42 family according to MEROPS database [14].

Glutamyl aminopeptidase PepA, which belongs to the M42 family, has been reported to show substrate specificity toward acidic amino acids at the N-terminus [15]. Although the crystal structure of glutamyl aminopeptidase from *Bacillus subtilis*, BsYsdC, which also belongs to the M42 family, has been determined [16], no information is available for the substrate specificity and the overall architecture. Here we report the crystal structure of PepA from *Streptococcus pneumoniae* (SpPepA). SpPepA forms dodecamer with tetrahedral architecture, exhibits selective substrate specificity to

Abbreviations: PepA, glutamyl aminopeptidase from *Streptococcus pneumoniae*; S1 pocket, substrate binding pocket 1; TRI, tricorn protease; PhTET1, PH0519 from *P. horikoshii*; PhTET2, PH1527 from *P. horikoshii*; PhTET3, PH1821 from *P. horikoshii*

* Corresponding authors. Fax: +82 31 290 7015 (S. Lee), +82 31 299 6159 (K.K. Kim).
E-mail addresses: sangholee@skku.edu (S. Lee), kkim@med.skku.ac.kr (K.K. Kim).

0006-291X/$ - see front matter © 2009 Elsevier Inc. All rights reserved.
doi:10.1016/j.bbrc.2009.11.075

acidic amino acids with the preference to glutamic acid. The substrate binding S1 pocket contains Arg-257 which allows electrostatic interactions with the N-terminal acidic residue in the substrate.

Materials and methods

Cloning, expression, and purification. Gene encoding the PepA of *S. pneumoniae R6* (GeneID: 15903724) was amplified by PCR from *S. pneumoniae R6* genomic DNA and cloned into a pET-based vector with a tobacco etch virus (TEV) protease cleavable N-terminal hexa-histidine tag. The recombinant plasmid, named pVFT1S-PepA, was transformed into *Escherichia coli* (*E. coli*) BL21 (DE3) cells (Novagen). Cells were cultured in Luria Bertani medium at 37 °C to an OD_{600} of 0.5 before inducing with 0.5 mM isopropyl-β-D-thiogalactopyranoside. The protein was first purified by metal affinity chromatography on a HiTrap™ chelating column (GE Healthcare). The N-terminal His-tag was removed using TEV protease in buffer A (20 mM Tris–HCl, pH 7.5, and 10 mM NaCl). The cleaved protein was further purified by anion exchange chromatography on a HiTrap™ Q column (GE Healthcare). The purified protein was dialyzed against buffer B (20 mM Tris–HCl, pH 7.5) and concentrated using YM-3 ultrafiltration and Centricon (Millipore). The protein concentration was estimated by the Bradford method.

Crystallization and data collection. Initial crystallization was performed at 20 °C by microbatch method. 1 μl of protein solution at 20 mg/ml in 20 mM Tris–HCl, pH 7.5, was mixed with the same volume of for the commercial crystal screening solutions for initial screening. Each drop was covered by 10 μl of Al's Oil (Hampton Research). The best crystals were obtained by increasing the protein concentration to 25 mg/ml and the reservoir condition was as the following: 33% PEG 8000, 20 mM sodium cacodylate, pH 6.5, and 50 mM ammonium sulfate. Initial diffraction experiments were performed at the 4A beamline of Pohang Accelerator Laboratory, Korea. Diffraction data were collected at the AR-NW12 beamline in Photon Factory, Japan. All data were processed by *HKL2000* [17]. Details about data processing are listed in Table 1.

Structure determination. The structure of SpPepA was determined by molecular replacement. Initial partial solution was obtained by *MOLREP* [18] using the monomeric structure of BsYsdC (PDB ID: 1VHE) as a search model. However, the presence of multiple copies of the molecule in the asymmetric unit hindered us to locate all the 12 monomers in the asymmetric unit when using the monomer as the search model. The results from size exclusion chromatography suggested that SpPepA would be dodecamer in solution (data not shown). Based on such data, we assumed that SpPepA would form a tetrahedron just like the search model. We then constructed the tetrahedral search model by applying crystallography symmetry operations, leading us to the solution. Rigid body refinement of the initial solution and density modification were performed using *REFMAC* [19] and *DM* [20], respectively. Iterative model building was done using *COOT* [21]. Refinement was performed by applying non-crystallographic symmetry restraints using *REFMAC*. The final model contains all residues except residues 1–2 and 117–131 due to poor electron densities in these regions. The active site metals are modeled as zinc ions. Final refinement statistics are given in Table 1. The quality of the structure was checked using *PROCHECK* [22]. All structural figures were generated using *PyMOL* [23].

Aminopeptidase activity assay. Aminopeptidase activity of SpPepA was measured using 12 aminoacyl-*para*-nitroanilides (aminoacyl-*p*NA) substrates (Glu, Asp, Ala, Arg, Met, Lys, Val, Pro, Phe, Leu, His, and Ile). For each experiment, 500 μM of a substrate was mixed with 2 μM of the purified SpPepA in a buffer (20 mM Tris–HCl, pH 7.5, and 100 μM $ZnCl_2$). The release of each aminoacyl-*p*NA was then monitored on a spectrophotometer at wavelength 405 nm every 5 min, up to 40 min. The activity of SpPepA for the Glu-*p*NA substrate was set to 100% and the relative activities of other substrates were calculated.

Table 1
Data collection and refinement statistics.

Unit cell parameters	
Space group	$P2_1$
Unit cell	a = 138.3 Å
	b = 118.3 Å
	c = 160.3 Å
	β = 106.4°
Data collection	
Beamline	NW12A, Photon Factory
Resolution range (Å)	50.0–2.7 (2.8–2.7)[a]
No. observations	520,491
No. unique reflections	137,138
Completeness (%)	99.9 (99.3)[a]
R_{merge} (%)[b]	10.4 (39.0)[a]
I/σ (I)	11.5 (2.4)[a]
Refinement	
Resolution range (Å)	44.4–2.7
No. reflections working set	130,226
No. reflections test set	6890
No. protein atoms	30,744
No. waters	549
No. metal ions (zinc)	24
R_{work}/R_{free} (%)[c]	20.0/24.7
R.m.s.d. bond lengths/angles (Å)	0.008/1.238
Average B-factor (Å^2)	28.1
Ramachandran plot (%)[d]	97.2/2.7/0.1

[a] The value in parentheses of resolution range, completeness, R_{merge} and $I/\sigma(I)$ correspond to the last shell.
[b] $R_{merge}(I) = \sum_{hkl}\sum_j|I(hkl)_j - I(hkl)|/[\sum_{hkl}I_{hkl}]$, is the jth measurement of the intensity of reflection hkl and $<I(hkl)>$ is the averaged intensity.
[c] $R = \sum_{hkl}||F_{obs}| - |F_{calc}||/\sum_{hkl}|F_{obs}|$, where R_{free} is calculated without a s cutoff for a randomly chosen 5% of reflections, which were not used for structure refinement, and R_{work} is calculated for the remaining reflections.
[d] Percentage of residues in favored region/allowed region/outlier region.

Results and discussion

Subunit structure

The structure of SpPepA subunit consists of three domains: two dimerization domains and one proteolytic domain (Fig. 1A). The dimerization domain I is composed of three short α-helices and five anti-parallel β-sheets; the dimerization domain II of long loops and two-stranded anti-parallel β-sheets; and the proteolytic domain of eight stranded anti-parallel β-sheets surrounded by eight α-helices. The subunit structure of SpPepA is consistent with those belonging to the M42 family. For example, the subunit structure of SpPepA is well superposed with that of BsYsdC (PDB ID: 1VHE) as evidenced by r.m.s. deviations of 1.1 Å for 308 Cα atoms.

Active site is located in the proteolytic domain and the active site residues are well conserved among M42 proteases (Fig. 2). The residues coordinating metals are well conserved in SpPepA: His-66, Asp-181, Glu-214, Asp-236, and His-318. We modeled two zinc ions in the active site based on electron densities contoured at up to 3σ level although the presence of the zinc ions in the crystal was not confirmed (Fig. S1). The distance between two zinc ions is 3.4 Å, which is consistent with the distances in other zinc-containing proteases showing similar subunit folds: for example, 2.9 Å for bovine lens leucine aminopeptidase [24] and 3.5 Å for aminopeptidase from *Aeromonas proteolytica* [25].

Oligomeric structure

Structural and biochemical data support that the overall architecture of SpPepA is a tetrahedron as a dodecamer, which is a

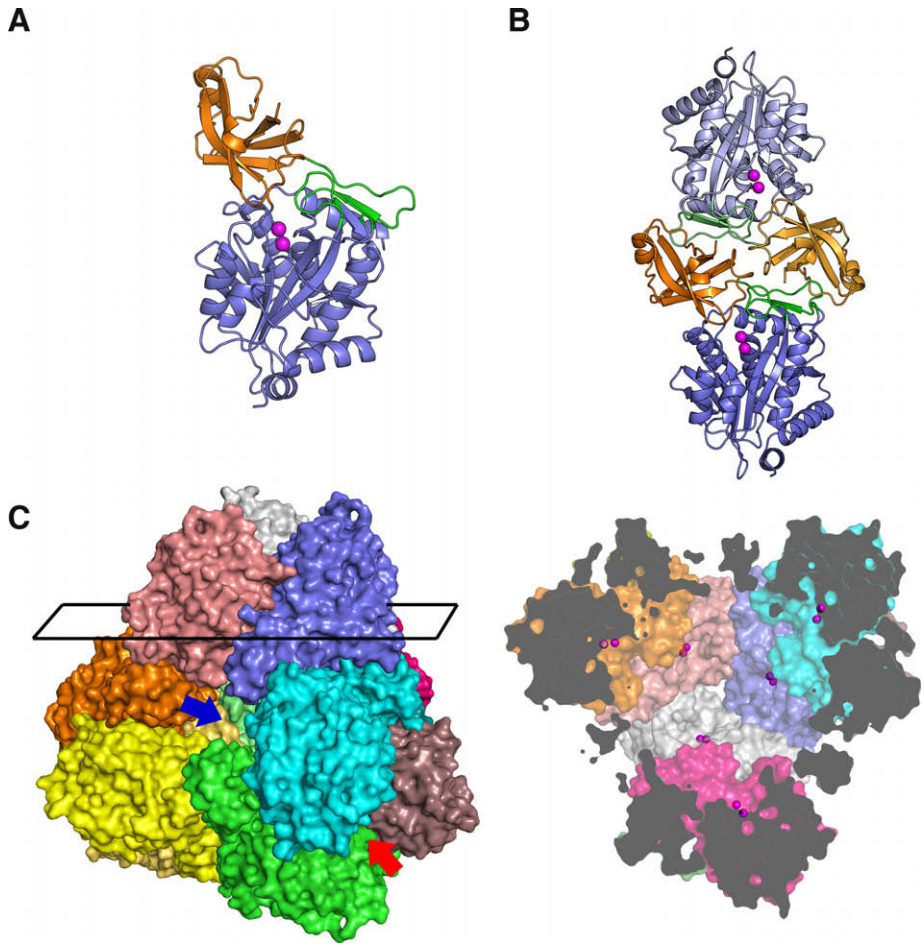

Fig. 1. Crystal structure of SpPepA. (A) Monomer structure. Dimerization domains I, II, and catalytic domain are colored orange, green, and blue, respectively. Two zinc ions are represented by magenta spheres. (B) Dimer structure. The three domains (dimerization domains I and II and proteolytic domain) of the second monomer are colored light orange, light green and light blue, respectively. (C) Tetrahedral architecture formed by dodecamer. Each monomer is colored differently. (Left) Surface representation of the dodecamer. The wide and the narrow channels are indicated by blue and red arrows, respectively. (Right) Cross-section of the black rectangle in the left panel. The zinc ions are shown as magenta spheres. (For interpretation of the references to color in this figure legend, the reader is referred to the web version of this article.)

shared structural feature among TET proteases (Fig. 1C). The SpPepA crystal contains 12 identical subunits in the asymmetric unit. Two subunits form a dimer via the two dimerization domains (Fig. 1B), which in turn constructs a tetrahedron. Subunit interactions are mainly formed by two dimerization domains and include electrostatic and hydrophobic interactions. Additional subunit interactions are found at the edge of the tetrahedron where the proteolytic domains from three subunits are held together. The results from size exclusion chromatography strongly suggest that SpPepA exits as a dodecamer in solution (data not shown). Electron microscopic studies revealed that SpPepA forms a TET-like structure (Fig. S2). Dimension of the tetrahedron observed under the microscope matches well with that from the crystal structure. In the case of BsYsdC for which the subunit structure is known, no biochemical data about the oligomeric state in solution are available [16]. Our results suggest that BsYsdC also exits as a dodecamer in solution considering the high sequence identity (37%) and the similarity of the subunit structure to SpPepA.

The tetrahedral architecture of SpPepA reveals a cavity at the center with four wide channels and four narrow ones (Fig. 1C). The wide channels are located on the faces of the tetrahedron and the narrow ones on the edges. The active sites are then aligned around the central cavity. Previous studies have revealed the same architecture for the TET family members and suggested that the wide channels are used for substrate entry and the narrow ones for substrate exit [8,10]. The diameter of the wide channel is 20 Å, compatible with that of the wide channel in HmTET [8]. The size of the substrate entry channel and the localization of the active site inside the tetrahedron obviously limit the substrates by their lengths.

Substrate specificity

Substrate binding pocket of SpPepA is constructed by Asp-236, Ser-238, Leu-255, Arg-257, Thr-309, and Gly-311 (Fig. 3A). Arg-257 is notable because the position of Arg-257 side chain creates a positive patch in the S1 pocket (Fig. 3B). Therefore, the positive patch of SpPepA appears to be responsible for its specificity toward acidic amino acids in the S1 position. The S1 pockets of PhTET2, PhTET3, and BsYsdC show negative patches. The negative patch in the S1 pocket of PhTET3 appears to confer the substrate specificity toward lysine, a basic amino acid [13]. In the case of PhTET1, the S1 pocket exhibits a weak negative patch. The inhibitor amastatin is aligned in the active site of PhTET1 by its electrostatic potential, implicating that the substrate specificity of PhTET1 is correlated with the charge distribution in the S1 pocket [10]. The positive patch in the S1 pocket is a distinct feature when compared to the S1 pockets of other TET protease structures (Fig. 3C). Some other TET proteases apparently harbor basic residues corresponding to Arg-257 in SpPepA (Fig. 2). However, it appears that the specific

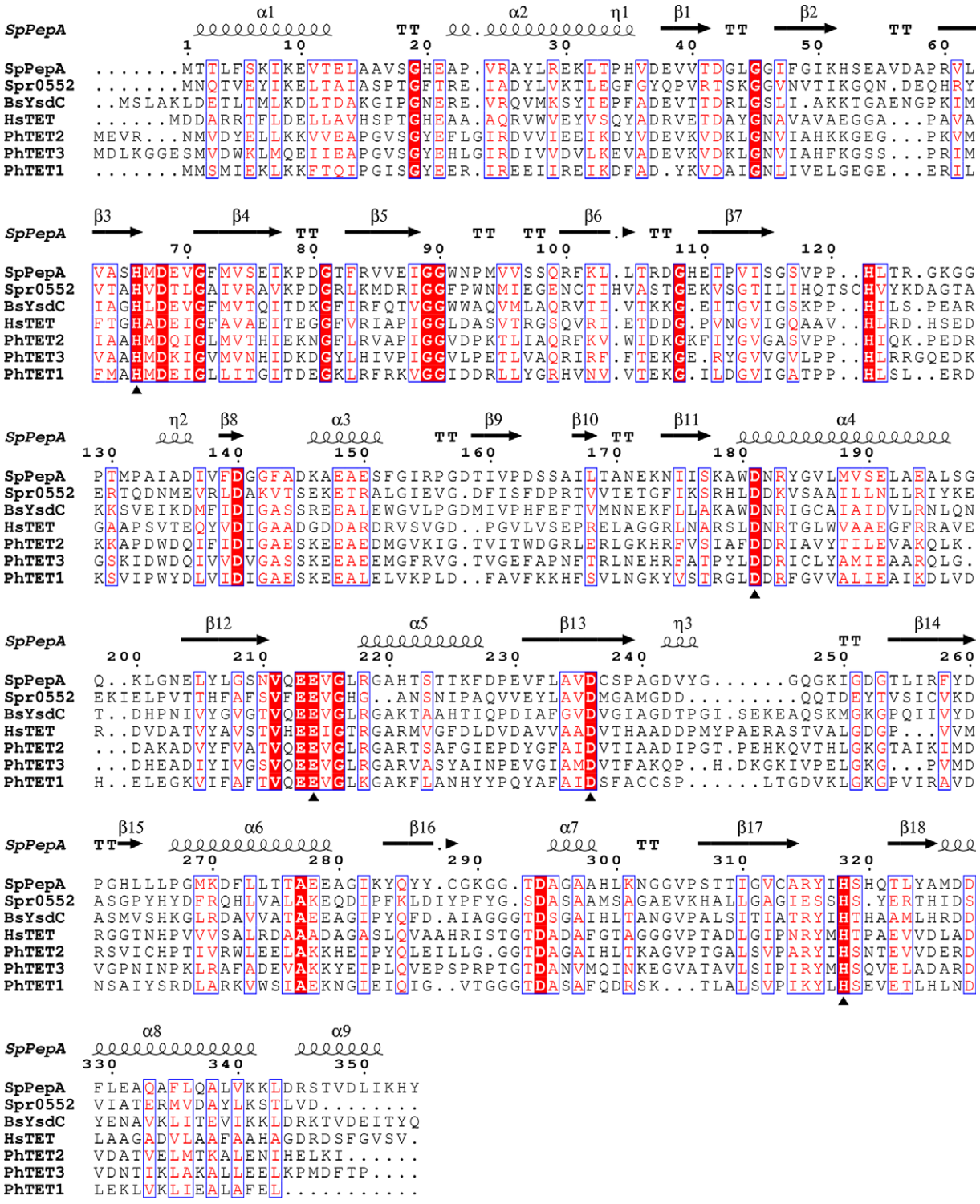

Fig. 2. Structure-based multiple sequence alignment of M42 family proteases. SpPepA: gluamyl aminopeptidase from *S. pneumoniae*; Spr0552, a hypothetical protein from *S. pneumoniae*; BsYsdC: Glutamyl aminopeptidase from *B. subtilis*; HsTET: endoglucanase from *Halobacterium sp. NRC-1*; PhTET2: PH1527 from *P. horikoshii*; PhTET3: PH1821 from *P. horikoshii*; and PhTET1: PH0519 from *P. horikoshii*. Secondary structure of SpPepA is shown at the top. Active site residues are represented by filled triangles at the bottom. Secondary structural elements are shown at the top of the sequences: α, helix; β, strand; η, 3_{10} helix; and T, turn.

conformation of the side chain may create differences in its electrostatic potential.

Modeling of the substrates into the binding pockets of the known TET protease structures supports the correlation between substrate specificity and charge distribution (Fig. S3). Glu-Ala dipeptide substrate is docked nicely into the binding pocket of SpPepA (Fig. S3A). The carboxylate group in the glutamic acid is juxtaposed to the positive patch in the S1 pocket, which can account for the substrate specificity of SpPepA toward acidic amino acids (Fig. S3B). By contrast, Lys-Ala dipeptide substrate fits well into the binding pocket of PhTET3, with the positive charge of the terminal amino group in the lysine pointing toward the negative charge developed in the S1

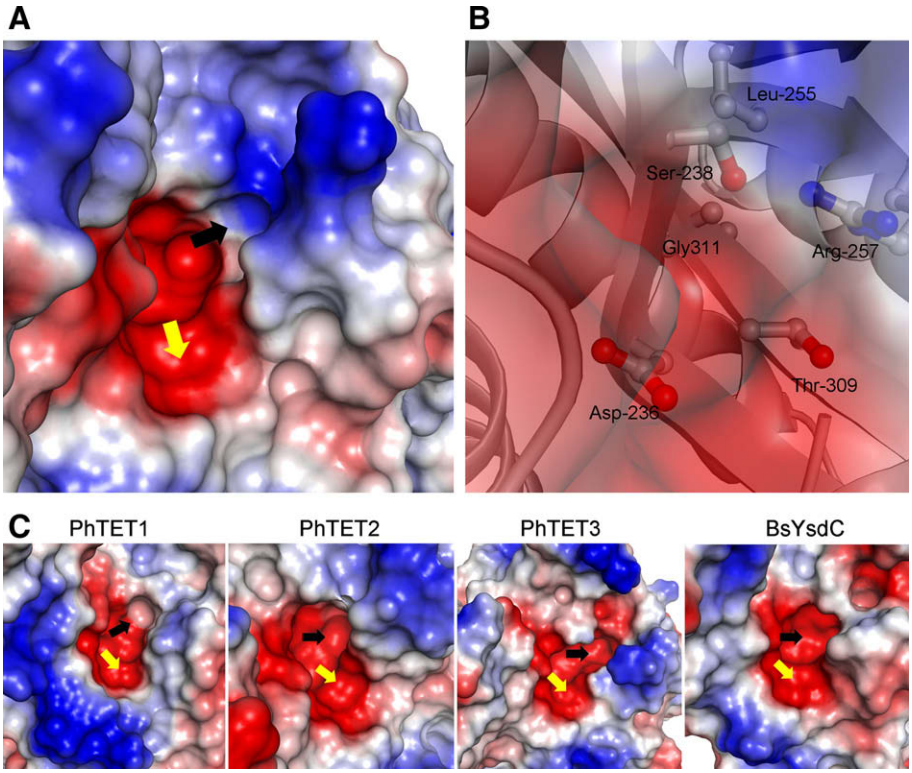

Fig. 3. Electrostatic potential surface of the substrate binding site of the M42 family proteases. (A) Electrostatic potential distribution surface of SpPepA. S1 and S1′ pockets are indicated by black and yellow arrows, respectively. (B) S1 pocket of SpPepA. Residues involved in substrate binding are represented by stick models. Electrostatic potentials are also shown. (C) Electrostatic potential surface of the substrate binding site from other M42 family proteases. S1 and S1′ pockets are indicated by black and yellow arrows, respectively. (For interpretation of the references to color in this figure legend, the reader is referred to the web version of this article.)

pocket (Fig. S3C). These results from modeling studies recapitulate the idea that the electrostatic charge is responsible for substrate specificities of the TET proteases.

Results from the activity assay using 12 aminoacyl-*p*NA substrates clearly demonstrate that SpPepA exhibits the strongest substrate specificity toward glutamic acid followed by aspartic acid (Fig. 4). The relative activity of aspartic acid is determined to be about 70% of glutamic acid, which can be understood in light of distance differences for the electrostatic interactions between Arg-257 and the carboxylate group in the P1 site of the substrate. Other amino acids tested exhibit little activity, consistent with the structural interpretation based on the electrostatic interactions. The results from the structural, computational and biochemical studies establish that the electrostatic interaction between Arg-257 in the S1 pocket and an acidic amino acid at the N-terminus of the substrate determines the substrate specificity of SpPepA. Our interpretation is compatible with a previous report claiming that only S1 and S1′ pocket of glutamyl aminopeptidase decide the coordination of substrates [26].

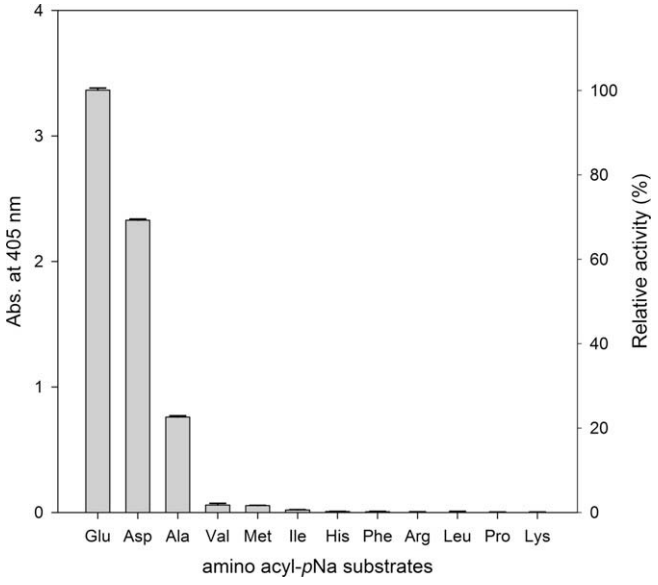

Fig. 4. Substrate specificity of SpPepA. Activity assays were performed with 12 aminoacyl-*p*Na substrates. Relative activities of the substrates used in the reference to glutamic acid are represented with error bars.

Multiple TET proteases are found with different substrate specificities in some prokaryotic genomes. In *P. horikoshii*, three TET proteases are present and their functions are distinguished by their substrate specificities. PhTET1 and PhTET2 show broad substrate specificities while PhTET3 presents substrate specificity toward lysine. In *S. pneumoniae*, only one TET protease – SpPepA – has been characterized, which raises the possibility that another TET protease is present with different substrate specificity. Interestingly, spr0552 gene encodes a hypothetical protein in *S. pneumoniae* which possesses sequence identity of 15% with SpPepA and conserved metal coordinating residues (Fig. 2). It is tempting to hypothesize that spr0552 might exhibit broad substrate specificity in *S. pneumoniae* just as PhTET1 and PhTET2 do in *P. horikoshii*.

TET proteases and TRI have been proposed to constitute evolutionarily divergent degradation mechanisms in bacteria and archaea [10]. Genomic analysis reveals that the two proteases exclude themselves in the genomes [12], suggesting that TET proteases and TRI are functionally redundant. TRI work together with at least three interacting factors but there is no known such factor for TET proteases. It is plausible that TET proteases ensure their substrate diversity by having multiple copies with different substrate specificities. If that is the case, TET proteases with broad

substrate specificities may perform housekeeping roles while those with selective substrate specificities might be involved in specific functions in a microorganism.

Streptococcus pneumoniae, a lactic acid bacterium (LAB), is one of major pathogens in children and elderly people causing pneumonia [27,28]. The observation that the expression level of SpPepA is decreased significantly in blood [29] implicates that the selective substrate specificity of SpPepA might play a role in the infection mechanism of *S. pneumoniae*, making further studies on the function of SpPepA more attractive.

Conclusions

We have determined the crystal structure of SpPepA, a glutamyl aminopeptidase, from *S. pneumoniae*. The structure of SpPepA shows canonical dodecameric tetrahedral architecture, characteristic of TET proteases. The substrate specificity of SpPepA is clearly towards acidic amino acids supported by both structural and biochemical data. The basic, positive patch formed by the non-conserved Arg-257 in the S1 pocket appears to be critical in mediating the selective substrate specificity with the acidic amino acid at the N-terminus of the substrate by electrostatic interactions.

Accession number

Atomic coordinates have been deposited in the Protein Data Bank, (PDB ID: 3KL9), www.rscb.org.

Acknowledgments

This work was supported by Faculty Research Fund, Sungkyunkwan University, 2007 and the Korea Research Foundation Grant funded by the Korean Government (MOEHRD, Basic Research Promotion Fund) (KRF-2008-314-C00224) to S. Lee and Ubiquitome Research Program (M10533010002-06N3301-00210) and 21C Frontier Functional Proteomics Program (FPR08B2-270) to K.K. Kim.

Appendix A. Supplementary data

Supplementary data associated with this article can be found, in the online version, at doi:10.1016/j.bbrc.2009.11.075.

References

[1] S. Gottesman, Proteolysis in bacterial regulatory circuits, Annu. Rev. Cell Dev. Biol. 19 (2003) 565–587.
[2] M. Kirschner, Intracellular proteolysis, Trends Cell Biol. 9 (1999) M42–M45.
[3] W. Baumeister, J. Walz, F. Zuhl, E. Seemuller, The proteasome: paradigm of a self-compartmentalizing protease, Cell 92 (1998) 367–380.
[4] S. Gottesman, M.R. Maurizi, Regulation by proteolysis: energy-dependent proteases and their targets, Microbiol. Rev. 56 (1992) 592–621.
[5] S. Gottesman, W.P. Clark, V. de Crecy-Lagard, M.R. Maurizi, ClpX, an alternative subunit for the ATP-dependent Clp protease of *Escherichia coli*. Sequence and in vivo activities, J. Biol. Chem. 268 (1993) 22618–22626.
[6] T. Tamura, N. Tamura, Z. Cejka, R. Hegerl, F. Lottspeich, W. Baumeister, Tricorn protease – the core of a modular proteolytic system, Science 274 (1996) 1385–1389.
[7] N. Tamura, F. Lottspeich, W. Baumeister, T. Tamura, The role of tricorn protease and its aminopeptidase-interacting factors in cellular protein degradation, Cell 95 (1998) 637–648.
[8] B. Franzetti, G. Schoehn, J.F. Hernandez, M. Jaquinod, R.W. Ruigrok, G. Zaccai, Tetrahedral aminopeptidase: a novel large protease complex from archaea, EMBO J. 21 (2002) 2132–2138.
[9] S. Russo, U. Baumann, Crystal structure of a dodecameric tetrahedral-shaped aminopeptidase, J. Biol. Chem. 279 (2004) 51275–51281.
[10] L. Borissenko, M. Groll, Crystal structure of TET protease reveals complementary protein degradation pathways in prokaryotes, J. Mol. Biol. 346 (2005) 1207–1219.
[11] M.A. Dura, V. Receveur-Brechot, J.P. Andrieu, C. Ebel, G. Schoehn, A. Roussel, B. Franzetti, Characterization of a TET-like aminopeptidase complex from the hyperthermophilic archaeon *Pyrococcus horikoshii*, Biochemistry 44 (2005) 3477–3486.
[12] G. Schoehn, F.M. Vellieux, M. Asuncion Dura, V. Receveur-Brechot, C.M. Fabry, R.W. Ruigrok, C. Ebel, A. Roussel, B. Franzetti, An archaeal peptidase assembles into two different quaternary structures: a tetrahedron and a giant octahedron, J. Biol. Chem. 281 (2006) 36327–36337.
[13] M.A. Dura, E. Rosenbaum, A. Larabi, F. Gabel, F.M. Vellieux, B. Franzetti, The structural and biochemical characterizations of a novel TET peptidase complex from *Pyrococcus horikoshii* reveal an integrated peptide degradation system in hyperthermophilic archaea, Mol. Microbiol. 72 (2009) 26–40.
[14] N.D. Rawlings, F.R. Morton, C.Y. Kok, J. Kong, A.J. Barrett, MEROPS: the peptidase database, Nucleic Acids Res. 36 (2008) D320–D325.
[15] K.J. l'Anson, S. Movahedi, H.G. Griffin, M.J. Gasson, F. Mulholland, A non-essential glutamyl aminopeptidase is required for optimal growth of *Lactococcus lactis* MG1363 in milk, Microbiology 141 (Pt 11) (1995) 2873–2881.
[16] J. Badger, J.M. Sauder, J.M. Adams, S. Antonysamy, K. Bain, M.G. Bergseid, S.G. Buchanan, M.D. Buchanan, Y. Batiyenko, J.A. Christopher, S. Emtage, A. Eroshkina, I. Feil, E.B. Furlong, K.S. Gajiwala, X. Gao, D. He, J. Hendle, A. Huber, K. Hoda, P. Kearins, C. Kissinger, B. Laubert, H.A. Lewis, J. Lin, K. Loomis, D. Lorimer, G. Louie, M. Maletic, C.D. Marsh, I. Miller, J. Molinari, H.J. Muller-Dieckmann, J.M. Newman, B.W. Noland, B. Pagarigan, F. Park, T.S. Peat, K.W. Post, S. Radojicic, A. Ramos, R. Romero, M.E. Rutter, W.E. Sanderson, K.D. Schwinn, J. Tresser, J. Winhoven, T.A. Wright, L. Wu, J. Xu, T.J. Harris, Structural analysis of a set of proteins resulting from a bacterial genomics project, Proteins 60 (2005) 787–796.
[17] Z. Otwinowski, W. Minor, Processing of X-ray diffraction data collected in oscillation mode, in: C.W. Carter Jr., R.M. Sweet (Eds.), Methods in Enzymology, vol. 276, Macromolecular Crystallography, Part A, New York, 1997, pp. 307–326.
[18] A. Vagin, A. Teplyakov, MOLREP: an automated program for molecular replacement, J. Appl. Crystallogr. 30 (1997) 1022–1025.
[19] G.N. Murshudov, A.A. Vagin, E.J. Dodson, Refinement of macromolecular structures by the maximum-likelihood method, Acta Crystallogr. D Biol. Crystallogr. 53 (1997) 240–255.
[20] K. Cowtan, dm: An automated procedure for phase improvement by density modification. Joint CCP4 and ESF-EACBM Newsletter on protein cyrstallography 31 (1994) 34–38.
[21] P. Emsley, K. Cowtan, Coot: model-building tool for molecular graphics, Acta Crystallogr. D Biol. Crystallogr. 60 (2004) 2126–2132.
[22] R.A. Laskowski, M.W. MacArthur, D.S. Moss, J.M. Thornton, PROCHECK: a program to check the stereochemical quality of protein structure, J. Appl. Crystallogr. 26 (1993) 283–291.
[23] W.L. DeLano, The PyMOL Molecular Graphics System. DeLano Scientific, Palo Alto, CA, USA, 2002.
[24] S. Burley, P. David, A. Taylor, W. Lipscomb, Molecular structure of leucine aminopeptidase at 2.7-Å resolution, Proc. Natl. Acad. Sci. USA 87 (1990).
[25] B. Chevrier, C. Schalk, H. D'Orchymont, J. Rondeau, D. Moras, C. Tarnus, Crystal structure of Aeromonase proteolytica aminopeptidase: a prototypical member of the co-catalytic zinc enzyme family, Structure 2 (1994).
[26] G.W. Niven, Gluamyl aminopeptidase (*Lactococcus*), in: A.J. Barrett, N.D. Rawlings, J.F. Woessner (Eds.), Handbook of Proteolytic Enzymes, second ed., Elsevier, London, 2004, pp. 965–968.
[27] M.R. Jacobs, *Streptococcus pneumoniae*: epidemiology and patterns of resistance, Am. J. Med. 117 (Suppl. 3A) (2004) 3S–15S.
[28] A. Ortqvist, J. Hedlund, M. Kalin, *Streptococcus pneumoniae*: epidemiology, risk factors, and clinical features, Semin. Respir. Crit. Care Med. 26 (2005) 563–574.
[29] S.M. Bae, S.M. Yeon, T.S. Kim, K.J. Lee, The effect of protein expression of *Streptococcus pneumoniae* by blood, J. Biochem. Mol. Biol. 39 (2005) 703–708.